LB-848

ELIMINATION OF MOIRÉ EFFECTS IN TRI-COLOR KINESCOPES

Property of
Albert E. Linden

RADIO CORPORATION OF AMERICA
RCA LABORATORIES DIVISION
INDUSTRY SERVICE LABORATORY

RADIO CORPORATION OF AMERICA
RCA LABORATORIES DIVISION
INDUSTRY SERVICE LABORATORY

LB-848

Elimination of Moiré Effects in Tri-Color Kinescopes

This report is the property of the Radio Corporation of America and is loaned for confidential use with the understanding that it will not be published in any manner, in whole or in part. The statements and data included herein are based upon information and measurements which we believe accurate and reliable. No responsibility is assumed for the application or interpretation of such statements or data or for any infringement of patent or other rights of third parties which may result from the use of circuits, systems and processes described or referred to herein or in any previous reports or bulletins or in any written or oral discussions supplementary thereto.

Approved

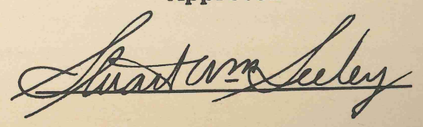

Elimination of Moiré Effects in Tri-Color Kinescopes

Introduction

Moiré effects which may arise in aperture mask tri-color kinescopes are spurious intensity variations in the picture in the nature of beat patterns between the scanning lines and the aperture array in the shadow mask. The visibility of these effects depends on the relative magnitudes of the scanning line width, mask aperture size, aperture spacing, and line separation, on the orientation of the scanning pattern relative to the mask, and, finally, on the picture content.

For the narrow aperture spacing normally employed (e.g., 215,000 apertures in a rectangular picture area of 104 square inches or 195,000 apertures in the somewhat smaller area defined by the framing mask) and for the preferred orientation of the scanning pattern, however, the moire effects are negligible. They may become noticeable, in the form of dot or bar patterns, if the aperture spacing is increased or the orientation of the scanning pattern relative to the mask is changed.

The variation in the line transmission of the mask indicates directly the degree to which the mask may distort transmitted intensity values. It increases with a reduction in the ratios of line width and aperture diameter to aperture spacing and with a departure from the preferred orientation of the scanning pattern relative to the mask. Again, for the preferred orientation and within the range of spot sizes required for optimum resolution, the variation in line transmission is negligible--one per cent or less. Furthermore, since the increase in the variation in transmission with departure from the preferred orientation is quadratic, the picture quality is insensitive to small deviations from the optimum orientation.

The Nature of the Moiré Introduced by the Mask

The introduction of the mask, with its regular hexagonal array of apertures, into the aperture mask tri-color kinescope[1] causes intensity variations in the image which are not present in a kinescope for monochrome reproduction. As long as these variations are limited to areas of the order of a picture element--as they would be, e.g., if the mask were simply bombarded by a uniform spray of electrons--they do not affect the picture; at the normal viewing distance the eye recognizes only the average brightness of a picture element and this, by assumption, is unaffected (in relative measure) by the mask.

[1] See H. B. Law, "A Three-Gun Shadow Mask Color Kinescope," *Proc. I.R.E.*, October 1951.

It will be shown that this condition applies also for actual television pictures which are formed by a set of equally spaced scanning lines, even though for uniform picture signal the intensity distribution on a kinescope screen, without mask, is not uniform. The brightness fluctuation, which is repeated identically for every line spacing, is greatest if the line width is small compared to the line spacing. Since, however, the latter lies close to the limit of visual resolution, this brightness fluctuation is scarcely perceived under normal circumstances.

The introduction of the mask, with its rows of apertures with a periodicity which differs, in general, from that of the scanning lines, will give rise to brightness fluctuations on the screen with a period which may be much greater than the spacing of either the mask aperture lines or the scanning lines. It will be assumed, to begin with, that scanning lines and mask aperture lines are aligned as shown in Fig. 1. Minimizing, in this manner, the vertical spacing of the mask-aperture lines serves to minimize the effect of the mask on vertical resolution and the prominence of spurious intensity fluctuations. The transmission of electrons through a row of apertures will be a maximum when a scanning line is centered on it; it will be least when its center line falls midway between two scanning lines. Thus, if, e.g., the spacing of the rows of apertures, $a/2$, is but slightly less than the line separation h the brightness of the field for uniform signal will be amaximum for the first condition and a minimum for the second, which will be reached $n-\frac{1}{2}$ scanning lines down the picture:

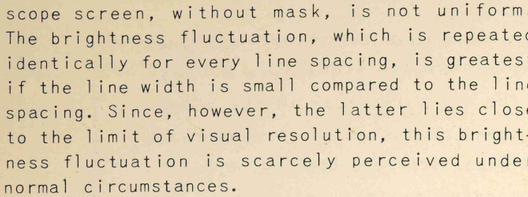

Fig. 1 – Preferred Orientation of Scanning Lines Relative to Mask.

$$(n - \tfrac{1}{2})\ h = \tfrac{1}{2}\ na; \qquad n = \frac{1}{2 - \frac{a}{h}} \qquad (1)$$

Hence there may be gross intensity fluctuations, or moiré, in the vertical direction with a period of $2n - 1$ scanning lines.

It is seen from Eq. 1 that the periodicity of the moiré is determined exclusively by the ratio of the dot separation a on the mask to the separation h of the scanning lines. The relative amplitude of the fluctuation, on the other hand, is determined only by the ratios of the line width d_s (for a given form of intensity distribution in the line) and the aperture diameter B to the line separation h.

If the scanning pattern is rotated relative to the mask by an angle θ, both the periodicity and direction of the moiré changes. Essentially, the intensity distribution in the field is given by the superposition of sinusoidal intensity variations of constant amplitude and differing frequency and direction. The amplitude is determined, as before, by the ratios of the line width and aperture diameter to the line separation. If the period of one of the sinusoidal components is much larger than that of any other, a line moiré, consisting of a sequence of broad bars, is obtained for uniform signal. If there are two components of nearly equal period, a dot moiré (with periods greater than the line separation) will be present.

The intensity distribution on the screen obtained for uniform signal does not, however, tell the full story of the effect of the mask on the picture. The picture signal contains, in effect, information regarding the variation in brightness of the sequence of equally spaced lines forming the scanning pattern. Hence, a proper measure of the error introduced by the mask is the variation in the transmission of the mask for these scanning lines, depending on the relative position of the scanning line and the aperture array in the mask. Fig. 2 compares schematically the intensity of a dot in a uniform-signal field and the line transmission. The dot intensity is the transmission

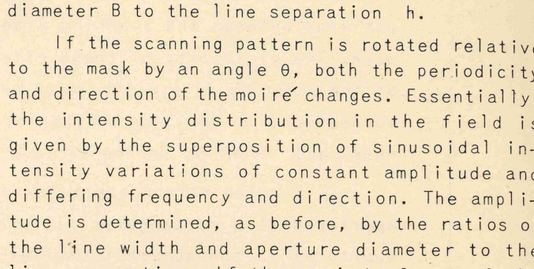

Fig. 2 – Schematic Representation of Dot Intensity and Line Transmission.

of a single mask aperture for the whole scanning pattern, whereas the line transmission is the transmission of the entire aperture mask for a single scanning line. The fluctuation in the dot intensity will be larger than that of the transmission as long as the spacing of aperture lines is less than the spacing of scanning lines; this condition is always satisfied in practice for the optimum orientation of the scanning pattern relative to the mask (Fig. 1).

This smaller fluctuation of the transmission is to be expected, since here electron current is, in effect, integrated over a coarser unit (the scanning line rather than the aperture line). In return for the greater coarseness of the information supplied, the transmission yields information not only regarding fluctuations in a uniform-signal field, but also for a field in which the line brightness may vary in some prescribed fashion (e.g., a succession of dark and light horizontal bars). If the scanning pattern is disoriented with respect to the mask, the transmission fluctuation rapidly increases, reaching a maximum for a displacement of 30 degrees relative to the optimum position; here the fluctuation in transmission greatly exceeds that in (dot) intensity for uniform signal, since the spacing of aperture rows (e.g., a = 0.023 or 0.030 inch) is materially greater than the scanning line spacing h (placed at 0.018 inch).

Basic Assumptions

The following calculations are made for a tube with a 9 x 12 inch scanning raster of 500 lines[2] and a line separation of 0.018 inch. A sequence of values, from 0.009 to 0.018 inch and from 0.0075 to 0.013 inch, are assumed for the line width d_s and the aperture diameter B. The separation of nearest neighbors in the aperture array, a, is made equal, in general, to 0.023 and 0.030 inch, although most of the results can readily be extended to any other values. The following exponential distribution is assumed for the scanning line:

$$f(y) = \frac{1}{b\sqrt{\pi}}\, e^{-y^2/b^2} = \frac{1.662}{d_s\sqrt{\pi}}\, e^{-(1.662y/d_s)^2} \qquad (2)$$

Here the "line width" d_s is defined as the transverse distance between two points at which the brightness of the line has dropped to $\frac{1}{2}$ of its maximum value. A "flat field" would correspond approximately to $d_s/h = 1$. The results reported here do not, of course, depend on the absolute dimensions of mask and scanning pattern, but only on the ratios d_s/h, B/h (or B/a), and a/h.

Intensity Distribution for Uniform Signal

The intensity transmitted by any one mask aperture may be written as a cosine series in terms of c/h, c being the distance between the center of the aperture and the center of the nearest scanning line:

$$I(c/h) = \frac{\pi B^2}{2\sqrt{3}a^2}\left(1 + \sum_{n=1}^{\infty} k_n \cos\frac{2\pi nc}{h}\right) \qquad (3)$$

Here, for convenience of comparison, the external coefficient has been set equal to the average transmission of the mask; in other words, the intensity falling on the total mask area per aperture has been set equal to unity. The values of k_n depend on the ratios of the line width and aperture diameter to the line separation, d_s/h and B/h. Tabulated below, they were calculated by the formulas derived in the Appendix.

Table I. Values of k_1

B in.		0.013	0.0115	0.009	0.0075	0
B/h		0.7222	0.6389	0.5	0.4167	0
d_s in.	d_s/h					
0.018	1	0.0277	0.0331	0.0416	0.0461	0.0576
0.0127	0.707	0.1631	0.1950	0.2450	0.2717	0.3394
0.009	0.5	0.3962	0.4732	0.5948	0.6596	0.8240

Table II. Values of k_2

B in.		0.013	0.0115	0.009	0.0075	0
B/h		0.7222	0.6389	0.5	0.4167	0
d_s in.	d_s/h					
0.018	1	$-1.5\cdot10^{-7}$	$-5\cdot10^{-6}$	$2.5\cdot10^{-7}$	$4.9\cdot10^{-7}$	$1.38\cdot10^{-6}$
0.0127	0.707	$-1.76\cdot10^{-4}$	$-5.9\cdot10^{-6}$	$3.02\cdot10^{-4}$	$5.9\cdot10^{-4}$	$1.66\cdot10^{-3}$
0.009	0.5	−0.00612	−0.00204	0.01045	0.02050	0.0576

[2] Or, e.g., a 8.45 x 11.27 inch raster of 470 lines. This refers to the raster on the mask. The picture area is some 5 per cent larger.

It is seen that even the second Fourier coefficient is quite insignificant, being 0.02 in the least favorable case considered. (The last column represents the Fourier coefficients of the intensity distribution without mask). Thus the intensity variation, as function of c/h, is practically sinusoidal and the relative amplitude of its fluctuations is given directly by the values of k_1.

Whereas the amplitude of the fluctuations is given by k_1, their periodicity in a vertical direction, for the alignment between aperture rows and scanning lines shown in Fig. 1, is given by Eq. 1. In particular for the values a = 0.030 in (a/h = 1,6667) and a = 0.023 in (a/h = 1.2778) the period of the fluctuation becomes 5 and 1.78 scanning lines. Since, in the second case, the period is of the same order as the dot separations, the effect would be here quite unnoticeable. With the larger spacing employed in some earlier experimental tubes a modulation of the vertical intensity should be readily visible even at viewing distance large enough that the line structure and the dot patterns are no longer resolved. It may be noted that, for the narrower spacing, a fluctuation with a somewhat larger period (1.99 h) is observed in a direction forming an angle of about 26 degrees with the vertical (see below).

The moiré for uniform signal when an angle θ is formed between the scanning lines and the x-axis (Fig. 1), which is imagined as fixed on the mask, is determined as follows: The intensity function I (Eq. 3) for the individual dot, with c replaced by y cos θ − x sine θ, is multiplied by a Fourier expansion which represents the array of the dot centers:

$$J(x, y; \theta) = \frac{B^2}{2\sqrt{3}a^2}\left[1 + \sum_{\substack{k,l=-\infty \\ k+l=2n \\ (k,l)\neq(0,0)}}^{\infty} k_1 \cos\frac{2\pi}{N_{kl}h}(x\cos\alpha_{kl} + y\sin\alpha_{kl})\right] \tag{5}$$

with

$$N_{kl} = \left[\left(\frac{kh}{a} + \cos\theta\right)^2 + \left(\frac{lh}{a\sqrt{3}} - \sin\theta\right)^2\right]^{-\frac{1}{2}} \tag{6}$$

and

$$\tan\alpha_{kl} = \frac{\frac{kh}{a} + \cos\theta}{\frac{lh}{a\sqrt{3}} - \sin\theta} \tag{7}$$

This represents the full solution for the intensity pattern obtained with uniform picture signal. The fluctuation components are all of the same amplitude k_1 but vary in the ratio N_{kl} of their period to the scanning line separation as well as in the direction of intensity variation α_{kl}; referred to the horizontal scanning lines this direction is $\alpha_{kl} - \theta$.

Only the terms of lowest order in h and k are significant since for higher order N_{kl} rapidly becomes small. Fig. 3 shows the variation of N_{kl} and $\alpha_{kl} - \theta$ as function of θ for the components which yield, for small values of θ, the largest values of N_{kl}. Here, again, it is assumed that a = 0.030 (a/h = 1.667) and 0.023 (a/h = 1.2778) inches.

$$J(x, y; \theta) = \frac{B^2}{2\sqrt{3}a^2}\left[1 + \sum_{n=1}^{\infty} k_n \cos\frac{2\pi n}{h}(y\cos\theta - x\sin\theta)\right]$$
$$\left[1 + 2\sum_{k=1}^{\infty}\cos\frac{4\pi k y}{a} + 2\sum_{l=1}^{\infty}\cos\frac{4\pi l x}{a\sqrt{3}} + 2\sum_{k,l=1}^{\infty}(1 + (-1)^{k+l})\cos\frac{2\pi k y}{a}\cos\frac{2\pi l x}{a\sqrt{3}}\right] \tag{4}$$

This formula assumes in effect that the intensity transmitted by each aperture is concentrated at the center of the corresponding dot. Since the dot size lies beyond the range of visual resolution this leads to no erroneous conclusions regarding any visible, macroscopic, intensity fluctuations. If the dot-structure

Transmission of Mask for a Scanning Line

The calculation of the transmission of the mask for a scanning line is indicated in detail in the Appendix. It is, of course, independent

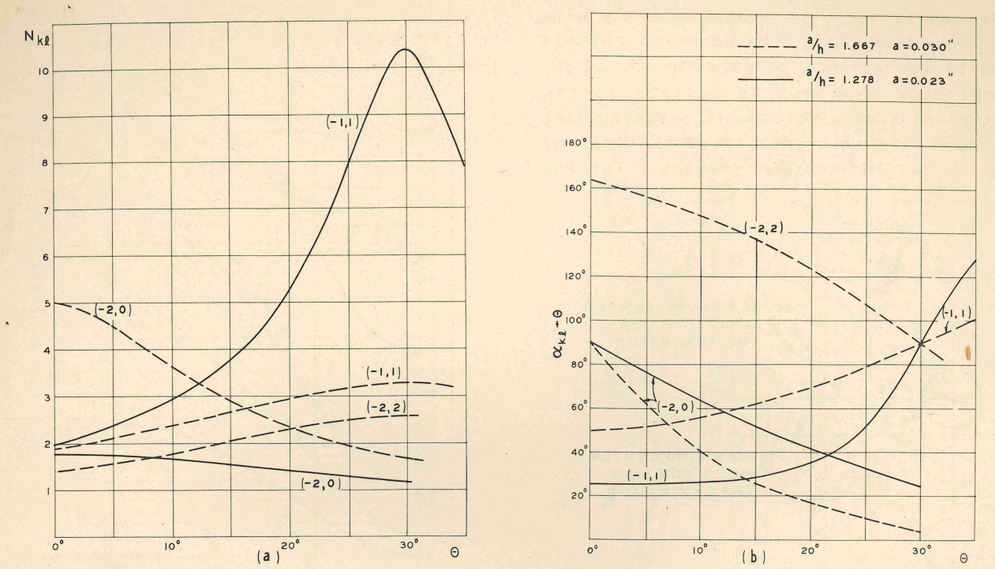

Fig. 3 – Variation (a) of Moiré Periods N_{kl} Measured in Multiples of the Scanning Line Separation and (b) of Directions of Corresponding Intensity Variations Relative to the Horizontal Scanning Lines as Function of Angle θ between Actual and Preferred Orientation of Scanning Lines Relative to Mask.

of h and, instead, a function of the two ratios B/d_s and B/a, namely of the ratios of the aperture diameter to the line width and the aperture separation. An amplitude factor k_T, corresponding to k_1 in Table I, may be introduced to describe the variation in transmission as the scanning line is displaced relative to the center line of a row of apertures by a distance varying from 0 to a/4. This factor is given, for comparison with Table I, in Table 3. It is also plotted, more extensively, in Fig. 7.

Table III. Values of k_T

a in.	B in. / d_s in.	0.013	0.0115	0.009	0.0075	0
0.030	0.018	0.004	0.005	0.008	0.007	0.012
0.030	0.01273	0.050	0.066	0.095	0.108	0.155
0.030	0.009	0.179	0.242	0.344	0.408	0.551
0.023	0.018					0.0003
0.023	0.01273		0.005	0.011	0.01	0.026
0.023	0.009		0.042	0.100	0.127	0.228

As already mentioned these fluctuation amplitudes are materially smaller than the values of k_1 listed in Table I. Identical values of k_T and k_1 are reached for a = 0.036 (a/2 = h), for which moiré effects are also most prominent, the period of the vertical intensity variation approaching infinity.

A plot of the actual transmissions as function of the aperture diameter B is given in Fig. 4.

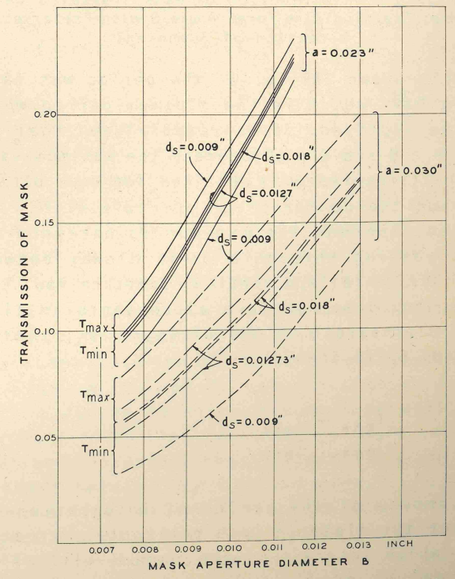

Fig. 4 – Maximum and Minimum Mask Transmissions as Function of the Mask Aperture Diameter.

The amplitude k_T increases rapidly with angular displacement of the scanning pattern relative to its optimum orientation (Fig. 1). This amplitude must now be defined as the fluctuation of transmission with scanning line displacement for some prescribed "period" of the mask in the x-direction (Fig. 5). For the

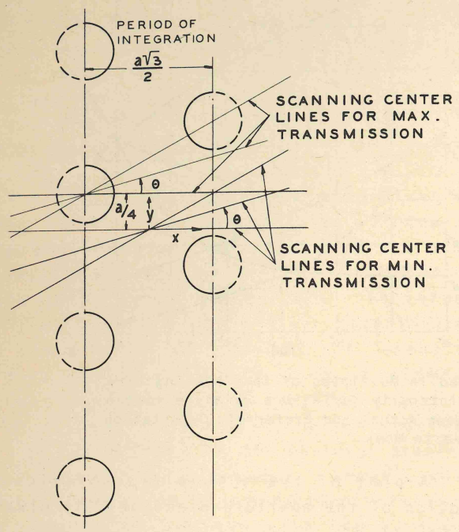

Fig. 5 – Determination of Mask Transmission When Scanning Line Forms Angle θ with Preferred Direction of Scanning.

results shown in Fig. 6, the period was taken to be $\frac{a\sqrt{3}}{2}$, which is the minimum period which may be employed. It is readily seen that for both θ = 0 and θ = 30 degrees the maximum value of the transmission is obtained for rays passing through the center of an aperture within the period, whereas the minimum is obtained for rays passing through a point midway between both horizontal and vertical aperture rows. The same should apply, to a close approximation, for intermediate values of angle. k_T, plotted in Fig. 6, is then given by

$$k_T = \frac{T_{max} - T_{min}}{T_{max} + T_{min}} \qquad (8)$$

The choice of the period of integration--in effect the distance in a horizontal direction over which intensities are summed--will affect the values of k_T only for angles between

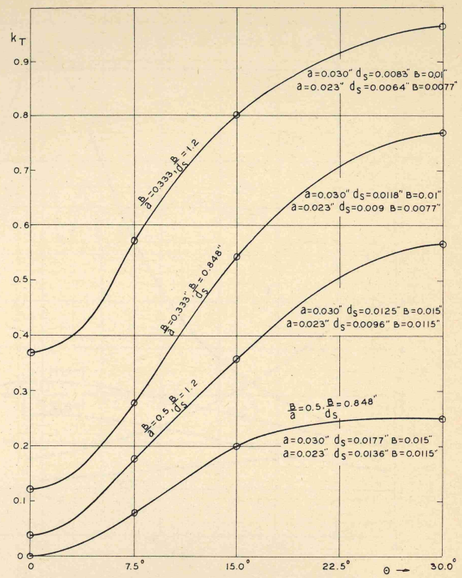

Fig. 6 – Fluctuation in Transmission as Function of Angle θ between Actual and Preferred Scanning Direction.

0 degrees and 30 degrees, not at the endpoints; the greater the period of integration, the less the fluctuation amplitude at intermediate points. The fluctuation amplitudes of the transmission for the endpoints, i.e., the most and the least favorable orientations of the scanning pattern (θ = 0° and θ = 30°), are plotted as function of the number of apertures in the picture area in Fig. 7.

Discussion of Results

The results for the moiré which is present with uniform signal are given by the data in Table I and Fig. 3. Table I shows that the amplitude of the moiré increases very rapidly as the scanning line is narrowed and more slowly, as the mask apertures are narrowed. For a scanning line width of 0.0127 inch and an aperture diameter of 0.009 inch, e.g., the modulation factor of the intensity is 0.25. With the larger aperture spacing (0.030 in.) this modulation has a period of 5 scanning line separations for the preferred orientation of the scanning pattern relative to the mask

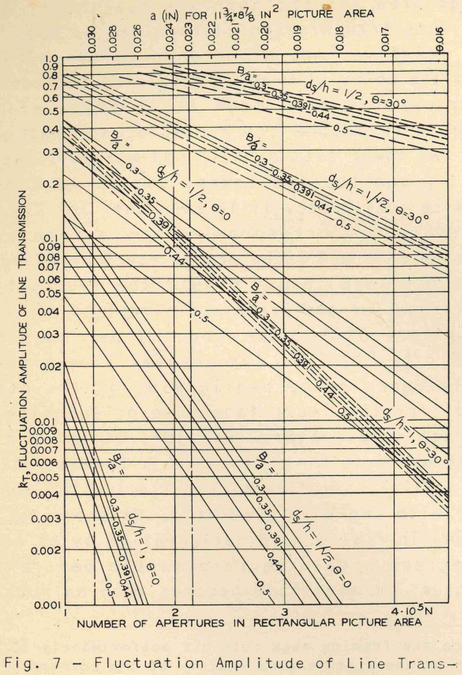

Fig. 7 – Fluctuation Amplitude of Line Transmission as Function of Number of Apertures in Mask.

(Fig. 1) line separations. The intensity variation is in the form of horizontal bars. In more detail, the intensity distribution given by the three terms with the largest periods in the range θ = 0 to θ = 30 degrees may be represented by an intensity contour pattern, such as that shown in Fig. 8. Not much weight can be attached to the finer structure of the pattern since the higher-frequency components of the intensity distribution have been omitted. The predominant importance of the term $N_{-2,0}$, with a vertical periodicity of 5 scanning line separations is, however, clearly evident.

As the scanning pattern is disoriented with respect to the mask, the system of horizontal bars also changes its orientation and contracts, eventually merging into a dot moiré with a periodicity of two to three line separations.

For the smaller aperture spacing (0.023 in.) the behavior is quite different. For the preferred orientation of the scanning pattern with respect to the mask, an unobjectionable dot moiré close to the limit of resolution (i.e.,

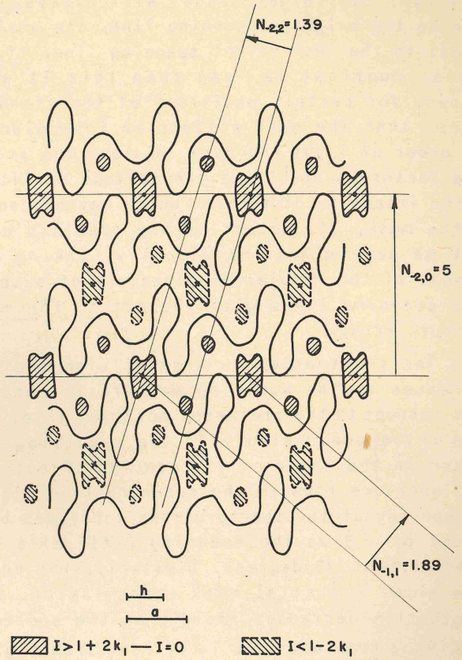

Fig. 8 – Approximate Intensity Contours for Uniform Signal, Computed for a/h = 1.667, θ = 0 from the Fourier Terms (-2,0), (-1,1), and (-2,2).

with periodicities of 2.0 and 1.8 scanning line separations) exists. With disorientation this gives way to a bar mosaic which reaches a maximum period of over 10 scanning line separations when the disorientation attains 30 degrees. Whereas, for uniform signal, the moiré pattern becomes less objectionable with disorientation for the tube with wide dot spacing, it is scarcely evident in the tube with narrow dot spacing unless there is a considerable departure from the preferred orientation.

The fluctuation in the transmission of the mask for a scanning line with vertical displacement of the line, as given by Table 3 and Figs. 4, 6, and 7, may serve as an index for the degree to which the mask permits the reproduction of fine (vertical) picture detail. In effect, it establishes a lower limit for the contrast between the picture signals for two scanning lines which will assure qualitatively correct reproduction. Thus if the ratio of the two picture signals (or, more precisely, the resulting beam currents) exceeds $(1 + k_T)/$

$(1 - k_T)$, the larger signal will always give rise to the brighter scanning line, the smaller signal to the less bright scanning line. If the signal contrast is less than this it will happen, for certain positions of the scanning lines, that the mask effects an inversion of the order of light and dark. Whereas the amplitude factor k_T specifies the maximum amplitude in the intensity distortion which may be caused by the mask, its extent in any specific case must be determined individually, taking due account of the regular displacement of successive scanning lines with respect to the mask aperture array.

The fluctuation in transmission rapidly increases as the scanning pattern is rotated with respect to the preferred position (Fig. 6). This corresponds simply to the resulting increase in the ratio of the spacing of successive aperture rows to the scanning line width; the spacing of the aperture rows increases by a factor of $\sqrt{3}$ as the scanning pattern is rotated through 30 degrees. Similarly, for equal line width and total mask transmission, the fluctuation decreases rapidly as the aperture spacing is reduced. This is evident from Fig. 7, where the fluctuation amplitude is plotted as function of the number N of apertures in the image area (or the aperture spacing a) with the mask transmission (determined by B/a) and the relative line width d_s/h as parameters. From the point of view of obtaining the maximum sharpness in the image it is pointless to lower d_s/h beyond $1/\sqrt{2} = 0.71$, so that only the two lower sets of full and broken lines in Fig. 7 and the two lowest curves in Fig. 6 need be considered. It is seen that for 215,000 apertures[3], corresponding to an aperture spacing of 0.023 inch, and an aperture diameter of 0.009 inch (B/a = 0.391) the fluctuation amplitude for the preferred direction of scanning ($\theta = 0$) is just about 1 per cent for $d_s/h = 1/\sqrt{2}$, less for greater line widths. It is hence quite negligible. On the other hand, for the least favorable orientation of the scanning pattern ($\theta = 30^\circ$) it is as much as 35 per cent for $d_s/h = 1/\sqrt{2}$. However, since the initial variation of the fluctuation amplitude with angle is quadratic, as shown by the curves in Fig. 6, a disorientation by at least 2 degrees should be permissible before the fluctuation amplitude becomes even as much as 2 per cent.

[3] Since the framing mask cuts off approximately 10 per cent of the picture area (mainly at the corners), the corresponding number of apertures contributing to the framed picture is 195,000.

E. G. Ramberg

Mathematical Appendix

Calculation of the Dot Intensity

If $I_o(c/h)$ is the intensity distribution of the scanning pattern for unit current falling on unit area,

$$I\left(\frac{c}{h}\right) = \frac{4}{a^2\sqrt{3}} \int_{-B/2}^{B/2} \sqrt{(B/2)^2 - y^2}\; I_o\left(\frac{y-c}{h}\right) dy \qquad (8)$$

with

$$I_o\left(\frac{y}{h}\right) = \frac{h}{b\sqrt{\pi}} \sum_{m=-\infty}^{m=\infty} e^{-\frac{(y + mh)^2}{b^2}}$$

$$= 1 + \sum_{n=1}^{\infty} a_{on} \cos \frac{2\pi n y}{h} \qquad (9)$$

$$= 1 + 2 \sum_{n=1}^{\infty} e^{-(\pi^2 n^2 b^2)/h^2} \cos \frac{2\pi n y}{h}$$

Substitution of Eq. 9 in Eq. 8 leads to

$$I\left(\frac{c}{h}\right) = \frac{\pi B^2}{2a^2\sqrt{3}} \left(1 + \frac{4}{\pi} \sum_{n=1}^{\infty} e^{-(\pi^2 n^2 b^2)/h^2} \int_{-1}^{1} \sqrt{1-s^2} \cos \frac{\pi n B s}{h}\, ds \cos \frac{2\pi m c}{h}\right)$$

$$= \frac{\pi B^2}{2a^2\sqrt{3}} \left(1 + \sum_{n=1}^{\infty} k_n \cos \frac{2\pi n c}{h}\right). \qquad (10)$$

The Fourier coefficient in this equation becomes:

$$k_n = 2e^{-(\pi^2 n^2 b^2)/h^2} \sum_{m=0}^{\infty} \frac{(-1)^m}{(m+1)\,(m!)^2} \left(\frac{\pi B n}{2h}\right)^{2m} \qquad (11)$$

Calculation of the Transmission

If the scanning pattern is in the preferred orientation (Fig. 1) relative to the mask, the transmission of the mask for the scanning line is given by

$$T\left(\frac{c}{a}\right) = \frac{2}{ab\sqrt{3\pi}} \sum_{n=-\infty}^{\infty} \int_{\frac{na-B}{2}}^{\frac{na+B}{2}} \sqrt{\left(\frac{B}{2}\right)^2 - \left(y - \frac{na}{2}\right)^2}\; e^{-\left(\frac{y-c}{b}\right)^2} dy$$

$$= \frac{2}{ab\sqrt{3\pi}} \sum_{n=-\infty}^{\infty} \int_{-B/2}^{B/2} \sqrt{\left(\frac{B}{2}\right)^2 - y^2}\; e^{-(1/b^2)\,(y-c+\frac{na}{2})^2} dy. \qquad (12)$$

A comparison of Eq. 12 with Eq. 8 shows that the transmission T is obtained from the dot intensity I if, in the latter, h is re-

placed by a/2. It follows, as already mentioned, that line transmission and dot intensity become identical for a = 2h.

For purposes of integration it is convenient to introduce the two variables

$$\beta = 2c/a \quad \text{and} \quad \alpha = [B/(2b)]^2 = (0.834B/d_s)^2.$$

Then Eq. 12 becomes

$$T\left(\frac{\beta}{2}\right) = \frac{B}{a}\sqrt{\frac{\alpha}{3\pi}} \int_{-1}^{1} \sqrt{1-s^2} \sum_{n=-\infty}^{\infty} e^{-\alpha\left(s-\beta+\frac{na}{B}\right)^2} ds \qquad (13)$$

If the scanning line is inclined by an angle θ to the preferred direction the transmission, calculated for the period shown in Fig. 5, becomes

$$T\left(\frac{\beta}{2}\right) = \frac{B}{a}\sqrt{\frac{\alpha}{3\pi}} \cos\theta \sum_{n=-\infty}^{\infty} \left[\int_{\frac{2na}{B}-1}^{\frac{2na}{B}+1} ds \int_{-\frac{\sqrt{3}a}{B}}^{-\frac{\sqrt{3}a}{B}+\sqrt{1-s^2}} d\xi + \int_{\frac{2na}{B}-1}^{\frac{2na}{B}+1} ds \int_{\frac{\sqrt{3}a}{B}-\sqrt{1-s^2}}^{\frac{\sqrt{3}a}{B}} d\xi \right]$$

$$\cdot e^{-\alpha[(s-\beta)\cos\theta - \xi\sin\theta]^2} \qquad (14)$$

with $s = \frac{2y}{B}, \qquad \xi = \frac{2x}{B}.$

This integral can be brought into a form convenient for quadrature by introducing polar coordinates with origin at the centers of the several apertures over which the integration is carried out. The result is:

$$T\left(\frac{\beta}{2}\right) = \frac{B}{2a}\sqrt{\frac{\alpha}{3\pi}} \cos\theta \left[\int_0^{\frac{\pi}{2}} \frac{d\varphi}{\sin^2\varphi} [F_1(\varphi) + F_1(-\varphi) + F_2(\varphi) + F_2(-\varphi)] \right.$$

$$\left. + \int_{\pi/2-\theta}^{\pi/2} \frac{d\phi}{\sin^2\varphi} [F_1(\varphi) - F_1(-\varphi) - F_2(\varphi) + F_2(-\varphi)] \right] \qquad (15)$$

with $F_j(\varphi) = \sum_{n=-\infty}^{\infty} \left[\frac{1}{\alpha} [e^{-\alpha q_{nj}^2} - e^{-\alpha(q_{nj}+\sin\varphi)^2}] \right.$

$$\left. + \sqrt{\frac{\pi}{\alpha}}\, q_{nj} [P(\sqrt{\alpha} q_{nj}) - P(\sqrt{\alpha}\,(q_{nj}+\sin\varphi))] \right]$$

$$q_{n1} = [\beta - \frac{2a}{B}(n+\tfrac{1}{4})] \cos\theta - \frac{\sqrt{3}}{2}\frac{a}{B}\sin\theta,$$

$$q_{n2} = [\beta - \frac{2a}{B}(n+\tfrac{3}{4})] \cos\theta + \frac{\sqrt{3}}{2}\frac{a}{B}\sin\theta,$$

$$P(y) = \frac{2}{\sqrt{\pi}} \int_0^y e^{-x^2} dx.$$